

Bendable Inorganic Thin-Film Battery for Fully Flexible Electronic Systems

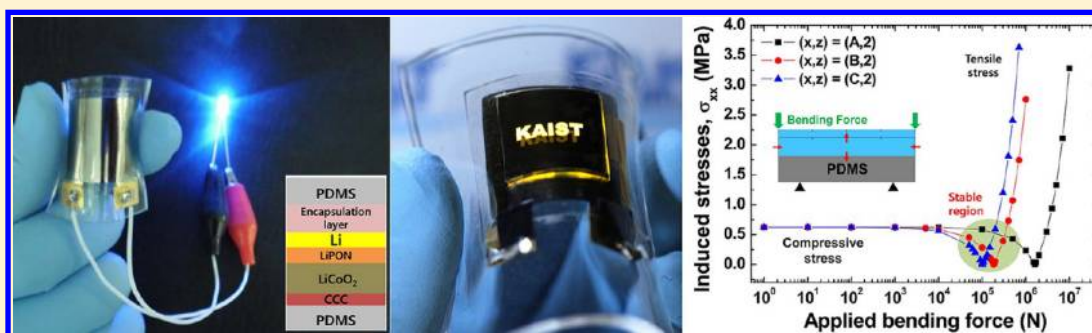
Min Koo,[†] Kwi-Il Park,[†] Seung Hyun Lee,[†] Minwon Suh,[†] Duk Young Jeon,[†] Jang Wook Choi,[‡] Kisuk Kang,[§] and Keon Jae Lee^{*†}

[†]Department of Materials Science and Engineering, Korea Advanced Institute of Science and Technology (KAIST), 291 Daehak-ro, Yuseong-gu, Daejeon 305-701, Republic of Korea

[‡]Graduate School of EEWS (WCU), Korea Advanced Institute of Science and Technology (KAIST), 291 Daehak-ro, Yuseong-gu, Daejeon 305-701, Republic of Korea

[§]Department of Materials Science and Engineering, Seoul National University, Gwanak-ro, Gwanak-gu, Seoul 151-742, Republic of Korea

S Supporting Information



ABSTRACT: High-performance flexible power sources have gained attention, as they enable the realization of next-generation bendable, implantable, and wearable electronic systems. Although the rechargeable lithium-ion battery (LIB) has been regarded as a strong candidate for a high-performance flexible energy source, compliant electrodes for bendable LIBs are restricted to only a few materials, and their performance has not been sufficient for them to be applied to flexible consumer electronics including rollable displays. In this paper, we present a flexible thin-film LIB developed using the universal transfer approach, which enables the realization of diverse flexible LIBs regardless of electrode chemistry. Moreover, it can form high-temperature (HT) annealed electrodes on polymer substrates for high-performance LIBs. The bendable LIB is then integrated with a flexible light-emitting diode (LED), which makes an all-in-one flexible electronic system. The outstanding battery performance is explored and well supported by finite element analysis (FEA) simulation.

KEYWORDS: Bendable thin-film battery, all-solid-state, rechargeable LIB, flexible electronic system

The advent of a fully flexible electronic system will be a great leap in technology, as it will open the door to the next-generation electronic environment based on bendable, implantable, and wearable devices. These next-generation electronic devices are marked by unprecedented advantages of excellent portability, lightweight, and conformal contact on curvilinear surfaces.^{1,2} Although the remarkable development of mechanically flexible electronic devices has been widely reported, their feasibility has been restricted in unit components, such as light-emitting diodes (LEDs),^{3,4} sensing electrodes,^{5,6} circuit elements,^{7–9} and radio frequency identification (RFID) antennas.¹⁰ Toward all-in-one flexible systems, the development of a bendable high-power source that can be applied to consumer electronics has been an obstacle to overcome.

Rechargeable lithium ion batteries (LIBs) have shown great promise as flexible power sources due to their high operating

voltage, high energy capacity, and long-term cyclability.^{2,11} In recent years, compliant materials on curvilinear surfaces, such as carbon nanotubes,^{12–15} carbon nanofibers,¹⁶ graphene,^{17,18} metal oxide-based nanowires,¹⁹ and slurry-typed mixtures of nanostructured active materials,^{20,21} have been explored as flexible LIB electrodes. Although they have shown advanced performance for flexible LIBs, the combination of these as anode or cathode has only been accessible to a few electrode materials that are synthesizable in certain nanostructures or carbon templates.²² Moreover, the use of liquid-type electrolytes has added more complexities in the realization of a fully flexible LIB, and their thermal stability should be carefully considered.^{23,24} In addition, the lightweight thin-film shape of

Received: June 15, 2012

Revised: July 27, 2012

Published: July 30, 2012

flexible LIBs required for nano/microelectromechanical systems (NEMS/MEMSs) cannot be formed by slurry-type composite materials.

In this paper, we developed a flexible LIB based on all-solid-state materials with an energy density, $2.2 \times 10^3 \mu\text{Wh}/\text{cm}^3$ at a rate $46.5 \mu\text{A}/\text{cm}^2$ (0.5 C) under polymer sheet wrapping, the highest energy density ever achieved for flexible batteries. The LIB properties as a function of the bending radius (R_c) show suitability for a high-performance flexible energy source. The stable energy density delivered on flexible substrates is well supported by theoretical studies and finite element analysis

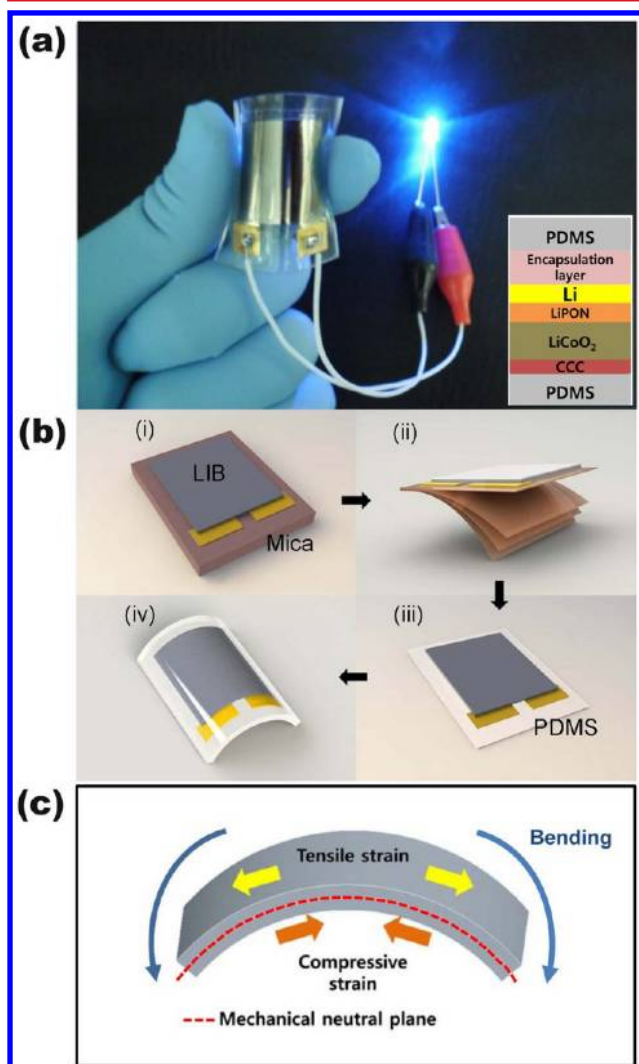


Figure 1. (a) Photograph of a bendable LIB turning on a blue LED in bent condition. The inset shows the stacked layers in the flexible LIB. (b) Schematic illustration of the process for fabricating flexible LIBs. A cultivated LIB on brittle mica substrate (i) is followed by mica substrate delamination using sticky tapes (ii), and then, the flexible LIB is transferred onto a PDMS polymer substrate (iii). Finally, the flexible LIB is covered with another PDMS sheet to enhance mechanical stability (iv). (c) Schematic image of the mechanical neutral plane generated from the counterbalance between tensile and compressive strain.

(FEA) simulation. Finally, a high-performance bendable thin-film LIB is then integrated into a flexible LED display system on a plastic substrate. As far as we know, this is the first prototype of a fully functional all-flexible electronic system.

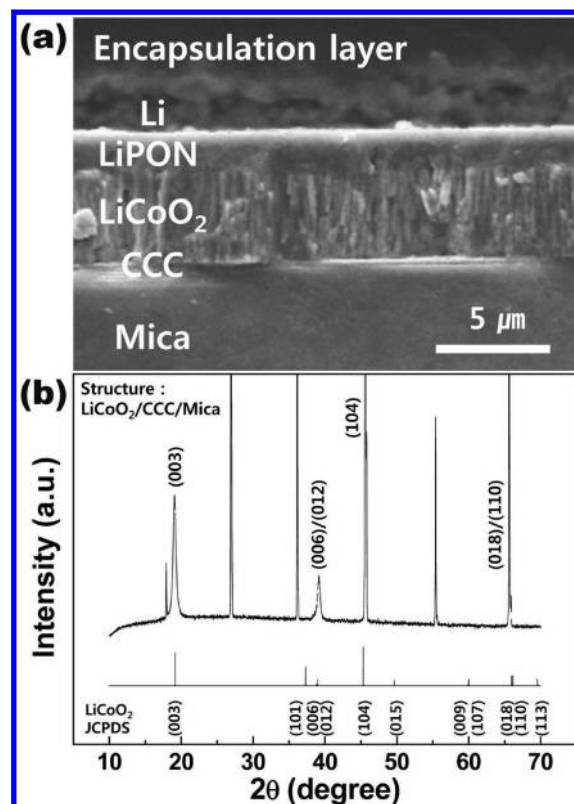


Figure 2. (a) Cross-sectional scanning electron microscope (SEM) image of a thin-film LIB on a mica substrate before substrate delamination. (b) A glancing incident X-ray diffraction pattern of the LiCoO_2 cathode material on a CCC/mica substrate.

Figure 1a shows the robustness of a flexible LIB turning on a blue LED in bent condition. The employment of high electrochemical potential materials, as depicted in the inset, leads to the maximum charging voltage of 4.2 V and the specific capacity of $106 \mu\text{Ah}/\text{cm}^2$ (discharge capacity of 683 μAh) at a rate of $46.5 \mu\text{A}/\text{cm}^2$ under polydimethylsiloxane (PDMS) polymer wrapping ($2.54 \times 2.54 \times 0.2 \text{ cm}^3$), which indicates higher performance than that of previously reported flexible LIBs based on nanosized materials.^{12–21} The construction of the bendable thin-film battery starts with a standard fabrication process upon a brittle mica substrate. A cathode current collector (CCC), a lithium cobalt oxide cathode (LiCoO_2 ; high-temperature (HT) annealing of LiCoO_2 at $700 \text{ }^\circ\text{C}$), a lithium phosphorus oxynitride electrolyte (LiPON), a lithium (Li) metal anode, and protective encapsulation multilayers were sequentially deposited on the substrate (Figure 1b-i). LiCoO_2 has received great interest from many researchers due to its high operating potential of $\sim 4 \text{ V}$ and high reversible capacity, and is currently the most widely used cathode in LIB.^{25–27} Although advanced cathode materials having high capacity and potential have been recently developed, LiCoO_2 is still regarded as the most reliable cathode material. As is the case for any other electrode materials, it should be noted that the HT annealing process for the crystallinity of LiCoO_2 material is a crucial step to realize the high-performance solid-state LIB. It is because the solid-state lithium diffusion is critically hindered by any imperfections in the crystal.

The next step is physical delamination of the mica substrate using sticky tapes (Figure 1b-ii). The mica material with weak-layered crystalline structure can be delaminated into thin sheets

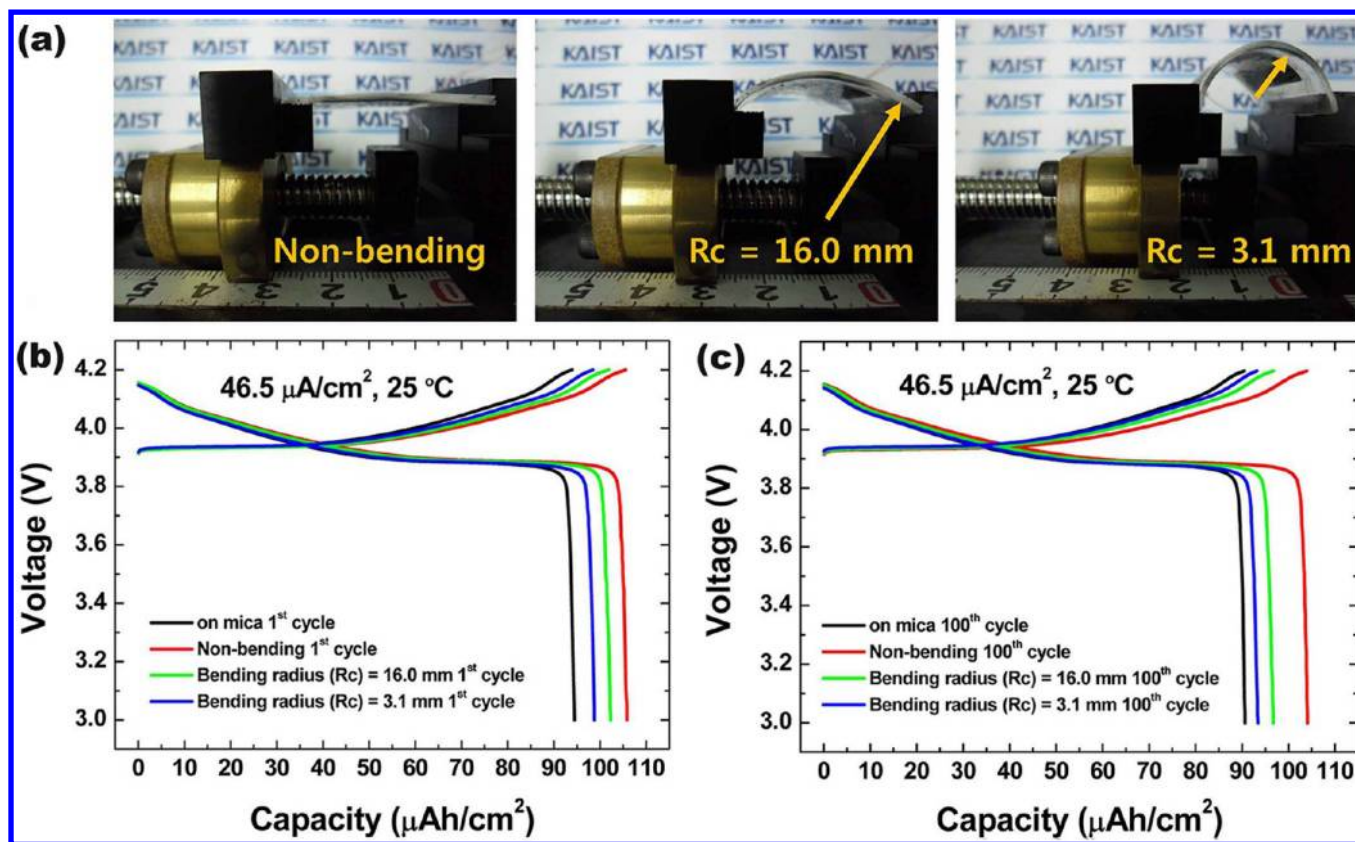


Figure 3. (a) Robustness tests of a flexible LIB on a bending stage machine. (b) Charge and discharge behavior of thin-film LIBs at the 1st cycle. (c) Charge and discharge curves at the 100th cycle.

by feeble peeling forces. Moreover, the intermolecular forces between layers of the mica substrate are weakened during the high-temperature annealing process. Therefore, the mica substrate can be easily removed even by the sticky tape without damaging the thin film LIB. The flexible LIB from substrate delamination is then transferred onto a PDMS polymer sheet (Figure 1b-iii), where the surface bondability of the PDMS helps the stable settlement of the flexible LIB. The final step is capping of the fabricated flexible LIB with another thin PDMS sheet to enhance its mechanical stability (Figure 1b-iv). The details of this process are presented in Figure S1 in the Supporting Information.

In this work, our transfer approach using mica substrate delamination enables the highly crystalline LiCoO_2 cathode thin film from HT annealing ($T_{\text{anneal}} \geq 700^\circ\text{C}$) for high-performance LIBs to be utilized on flexible polymer substrates ($T_{\text{glass}} \leq 150^\circ\text{C}$). Moreover, the thin-film active material in LIBs can be uniformly deposited upon mica substrates due to its ultraflatness property,^{28,29} which can considerably increase the possibility of LiCoO_2 's preferred orientation growth, resulting in reduced charge transfer resistance³⁰ of Li ions from the anode into the cathode and vice versa.

Stable electrochemical activity under mechanical flexibility is demonstrated in Figure 1a. This is due to the electrochemically active parts being located at the mechanical neutral plane (Figure 1c) formed by 1 mm thick PDMS capping shown in Figure 1b-iv. This protocol is similar to that of a stretchable and foldable electronic device previously reported by D.-H. Kim et al.³¹ While the film is bent as illustrated in Figure 1c, tensile strain arises on one outer side and compressive strain on the other inner side. Accordingly, the counterbalance between

these opposite strains develops a mechanical neutral space. The effects of the external PDMS sheet capping were analyzed by FEA simulation modeling (Figure S2, Supporting Information). The bending deformations correspond to uniaxial stresses σ_{xx} defined along the x -direction; $\sigma_{yy} = \sigma_{zz} = 0$.³² In this calculation, the PDMS capping can play a role in shifting of the mechanical neutral plane (Figure S2, Supporting Information), which the inorganic thin-film battery settles in. The reduction of induced stress σ_{xx} under 10 N bending forces reaches a maximum of 6.13% (i.e., 0.14 MPa) at $(x, z) = (0, 5)$ between LiPON and LiCoO_2 layers, where a contact resistance³⁰ may develop (Figure S3, Supporting Information).

A cross-sectional image of the thin-film LIB on a mica substrate is shown in Figure 2a. The employment of well-crystalline LiCoO_2 has been the focus of many studies on flexible LIBs based on plastic substrates with low thermal stability.^{33–35} However, the crystalline properties of LiCoO_2 produced by previously reported non-HT methods have not reached that of HT-annealed LiCoO_2 ($\geq 700^\circ\text{C}$). In Figure 2b, the glancing incident X-ray diffraction pattern of our LiCoO_2 cathode material shows the well-defined crystallinity from the optimization of the HT annealing process. The HT phase formation of the LiCoO_2 material through sufficient HT annealing treatment is especially important in order to avoid poor cycling and high self-discharge. The HT phase of the layered LiCoO_2 structure (space group $R3\bar{m}$) can be verified with (006), (012), (018), and (110) peak orientations.³⁶

Moreover, although the LIB with Li metal anode has a higher energy density than those with a carbon insertion anode,³⁷ recent studies of flexible LIBs have reported difficulty in carefully employing Li as an active material due to the danger of

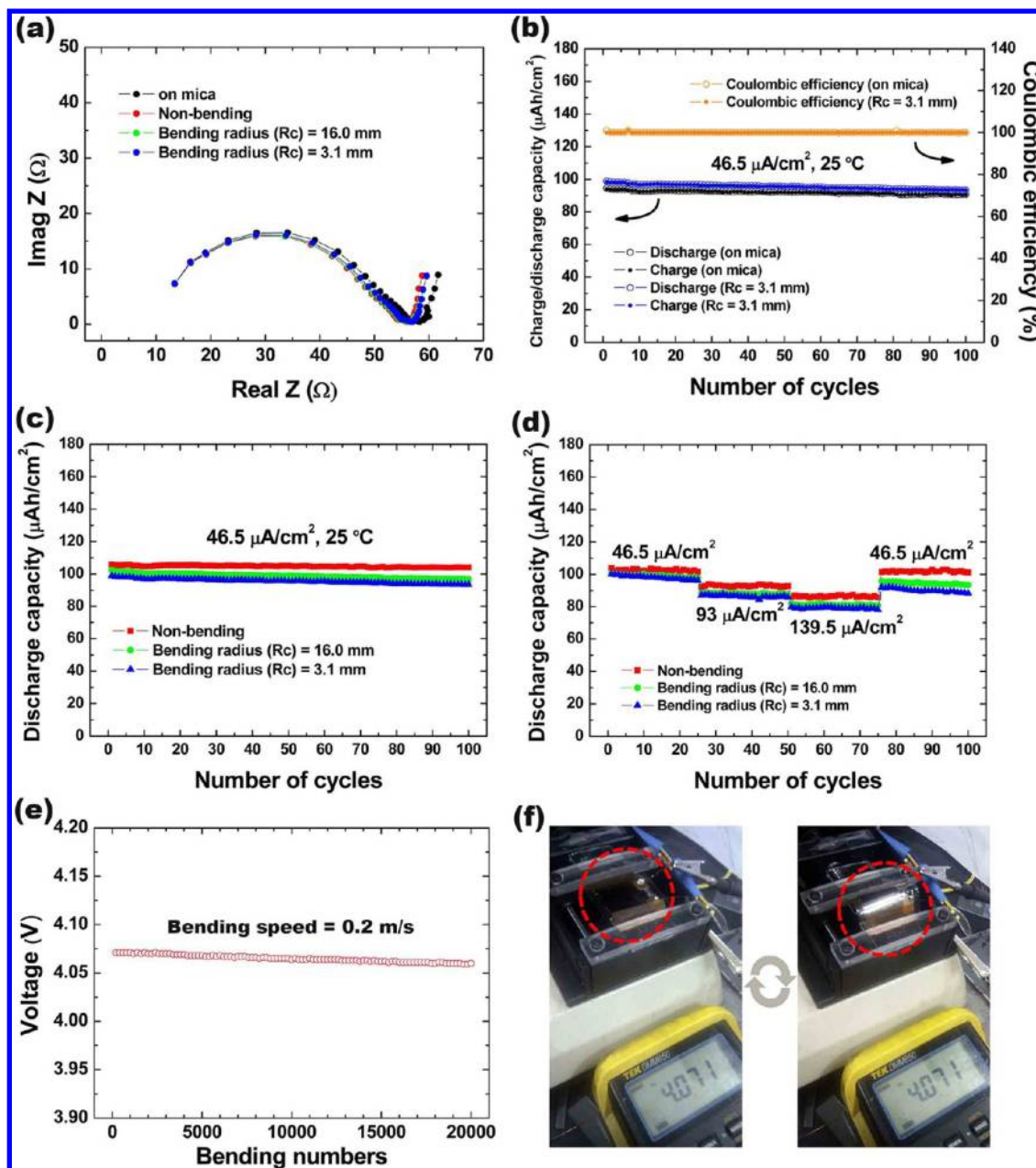


Figure 4. (a) Nyquist plots of AC impedance test measured at 5.0 V. An electrode had $18 \text{ mm} \times 18 \text{ mm}$ area. (b) Coulombic efficiencies of a flexible LIB bent to $R_c = 3.1$ mm and a mica LIB. (c) Capacity retention as a function of bending state at a constant current rate of $46.5 \mu\text{A}/\text{cm}^2$ during 100 cycles. (d) Capacity retention at various rates: 46.5 , 93 , and $139.5 \mu\text{A}/\text{cm}^2$. (e) Voltage retention during fatigue tests. (f) Demonstration of 1 cycle fatigue test: flat (left) and bent (right) state of the flexible LIB.

explosion. In our work, stable incorporation with Li anode using our transfer method after deposition in vacuum conditions enables the production of high-performance flexible LIBs on polymer substrates.

Figure 3a demonstrates robustness testing at various fixed bending radius conditions on a bending stage machine. The flexible LIB wrapped with two PDMS polymer sheets (1 mm in thickness) was bent from 2.5 mm ($R_c = 16.0$ mm) to 12.5 mm ($R_c = 3.1$ mm) compared with nonbending status ($R_c = \infty$). Even in the strain over a bending radius of 3.1 mm, we cannot observe any external damages (see the video S1 in the Supporting Information). At various bending radius values, Figure 3b and c show the charge and discharge profile during galvanostatic cycling tests at a rate of $46.5 \mu\text{A}/\text{cm}^2$ between 3.0

and 4.2 V. At the first cycle of the discharge curve in Figure 3b, it is interesting to note that the specific capacities of the flexible LIBs are enhanced as compared to $94 \mu\text{Ah}/\text{cm}^2$ for a mica LIB before substrate delamination, denoted as "on mica". Along with further increasing the degree of bending deformation on the flexible batteries, the specific capacity of $106 \mu\text{Ah}/\text{cm}^2$ for the nonbending unit on a flexible substrate is gradually decreased from the maximum value to $99 \mu\text{Ah}/\text{cm}^2$ at $R_c = 3.1$ mm. Figure 3c shows that the same tendency holds even at the 100th cycle.

This well-consistent reduction in specific capacity can be understood in terms of the charge transfer resistance of Li ions from and into the electrode including the contact resistance existing between LiPON and LiCoO_2 layers,³⁰ which are greatly

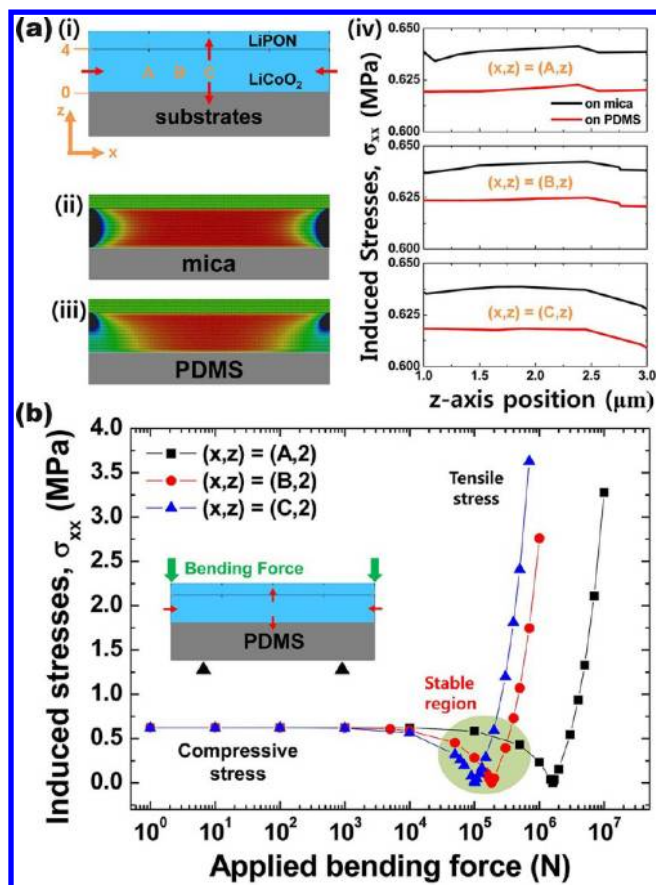


Figure 5. (a) FEA simulation geometry (i) for the correlation between substrate conditions and internal molar volume change stress. The stress distributions on mica (ii) and PDMS polymer (iii) substrates are compared, and the quantitative analysis of defined normal stress σ_{xx} (iv) is given. (b) Change of induced stresses as a function of applied bending force.

affected by the residual internal stresses of the flexible LIBs. Both of the resistances certainly give rise to overvoltage during charge and discharge, as shown in Figure 3b and c. The maximum of the overvoltage is observed for the composite on mica, while the minimum is given to the nonbending unit on the flexible substrate. The overvoltage thereafter increases with increased bending deformation. Note that the generation of overvoltage with the number of cycles and degree of bending deformation has the same tendency as that of charge density as seen in Figure 3b and c.

To further investigate the correlation between overvoltage and the degree of bending deformation, AC impedance was measured at 3.9 V by applying an AC-amplitude of 5 mV over the frequency range from 10^{-3} to 7×10^5 Hz at room temperature. The results are presented with various substrate conditions in Figure 4a. On the Nyquist plots of the AC impedance test, the high-frequency semicircles indicate the charge transfer resistance of Li ions including the contact resistance in LIBs. The highest impedance on the brittle mica substrate is considerably decreased by substrate delamination. However, the degree of bending deformation on the flexible polymer substrate further increases the impedance in arc size.

Therefore, it is deduced that the all-inclusive charge transfer resistance induced from residual stresses causes losses in the specific capacity of LIBs.³⁸ The residual stresses of sputter-deposited films on a mica substrate are gradually released upon

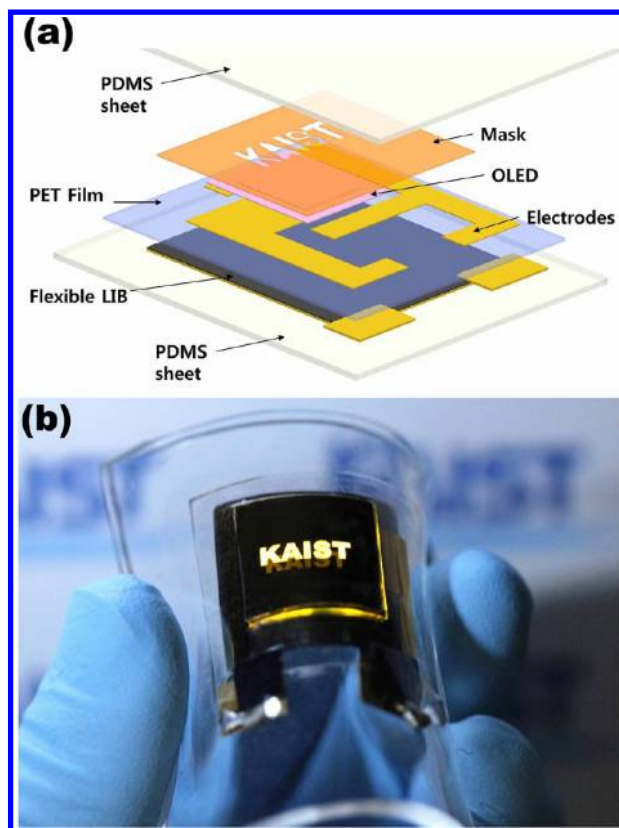


Figure 6. (a) Schematic diagram of an all-flexible LED system. (b) Picture of an all-in-one flexible LED system integrated with a bendable LIB.

the delamination of the mica layers, and then, the bending deformation can further increase the internal stresses.

This presumption can be developed from the analysis of residual stresses σ_f across a deposited film originating from Stoney's formula³⁹ given by

$$\sigma_f = \frac{E_s t_s^2 \delta}{3(1 - \nu_s) t_f r^2}$$

where E_s is the elastic modulus, t_s is the thickness, and ν_s is the Poisson ratio of the substrate; t_f is the thickness of the deposited film, and δ is the bending deflection at a distance r from the center of the substrate (see the Supporting Information for details).

In this analysis, the residual stress σ_f is parabolically and linearly increased with t_s and δ , respectively. In other words, the residual stresses can be considerably reduced by the mica substrate delamination, but they can also be enhanced by the degree of the substrate bending.

To evaluate the cyclability performance, the Coulombic efficiency of our flexible LIB being bent to $R_c = 3.1$ mm is compared with that of the mica LIB. As shown in Figure 4b, the Coulombic efficiency properties of the mica LIB and of the bent flexible LIB maintain their original capability over 99.8% even during 100 cycles. Figure 4c shows the capacity retention as a function of the degree of bending deformation at the constant current rate of $46.5 \mu\text{A}/\text{cm}^2$. After 100 cycles, the capacity retention for a nonbending condition on the flexible substrate is 98.4% of the original value, and those for $R_c = 16.0$ and 3.1 mm show a similar capacity retention of 94.5%. As shown in Figure 4d, the retention was measured at various

rates: 46.5 (0.5 C), 93 (1 C), and 139.5 $\mu\text{A}/\text{cm}^2$ (1.5 C). The discharge capacity for a nonbending condition retains 97.3% after 100 cycles. Those for $R_c = 16.0$ and 3.1 mm are 93.0 and 88.2%, respectively.

From Figure 4c and d, it is readily seen that the capacity retention is gradually aggravated by further bending progressing during 100 cycles of charge and discharge. It can be confirmed here that both contributions of the residual stresses caused by the degree of bending as well as the molar volume change in $\text{Li}_{1-d}\text{CoO}_2$ resulting during charge and discharge accelerate the degradation of the specific capacity of the LIB. Figure 4e shows the fatigue endurance of a flexible LIB under 2×10^4 bending cycles to $R_c = 3.1$ mm with a bending speed of 0.2 m/s. The endurance is evaluated with the voltage retention of the LIB. The initial delivered cell voltage of the flexible LIB of 4.071 V only decreases to 4.060 V, which just corresponds to 0.27% after 2×10^4 bending tests (Figure 4e). Figure 4f demonstrates the voltage retention during one bending cycle. The tested LIB is represented by two red dotted circles.

Detailed interpretation of the correlation between substrate conditions and molar volume change stress during 100 cycles of charge and discharge was carried out with FEA simulation. This calculation assumes that the lattice parameters of LiCoO_2 as a cathode material are $a = b = 0.282$ nm and $c = 1.41$ nm,⁴⁰ and then during charge and discharge cycling of a LIB, reversible Li extraction from and insertion into the cathode could lead to a change in composition to $\text{Li}_{0.62}\text{CoO}_2$, whose lattice parameters are $a = b = 0.28$ nm and $c = 2.93$ nm.⁴¹ The internal stresses arising from molar volume change are marked with red arrows in Figure 5a-i. Consequently, the stress distributions on mica and PDMS polymer substrates are depicted in Figure 5a-ii and a-iii. These results show that the capacities of LIBs transferred onto polymer substrates can be increased due to the prompt release of stresses by the molar volume change, which directly relates to the all-inclusive charge transfer resistance of Li ions. In addition, Figure 5a-iv presents the quantitative analysis of defined normal stress σ_{xx} along the x -direction. As shown in the results, the reduction of induced stresses due to the transfer onto PDMS substrate occurs at x -axis positions A, B, and C as well. The change in induced residual stresses is analyzed as a function of bending force in Figure 5b. The compressive stress due to molar volume change changes to tensile stress at a certain degree of bending deformation along with increasing bending force. It is expected that the point of the compressive to tensile transition may be the most stable state for flexible LIB operation. Therefore, it can be concluded that LIBs on flexible substrates can have higher stability and hence higher performance than those on brittle substrates.

Figure 6a gives a schematic outline of an all-in-one flexible LED system integrated with a bendable LIB. Gold electrodes deposited on a polyethylene terephthalate (PET) film connect the flexible LIB with an organic LED (OLED) fabricated by spin-coating and thermal evaporation methods on a flexible indium tin oxide (ITO) substrate (see the Supporting Information for details). The OLED backlight unit is covered with a letter-patterned shadow metal film. Finally, the wholly flexible LED system is wrapped with PDMS sheets to enhance its mechanical stability. The working system is demonstrated in Figure 6b.

We have fabricated an all-solid-state bendable LIB using a new universal transfer approach based on sacrificial mica substrates. The thin-film LIB is capable of a maximum 4.2 V charging voltage and 106 $\mu\text{Ah}/\text{cm}^2$ capacity, which indicate the

highest performance ever achieved for flexible LIBs. Moreover, its volumetric energy density can be considerably enhanced by reducing the dead volume such as external PDMS sheets. The evaluation tests and the simulation results show the effects of residual stress release from substrate delamination. Our bendable LIB enables the fabrication of an all-in-one flexible LED display integrated with a bendable energy source, which provides an innovative platform for the next-generation flexible electronic system. This novel transfer approach can be expanded to various high-performance flexible applications, such as thin-film nanogenerators,^{42,43} thin-film transistors (TFTs),⁷ and thermoelectric devices. We are currently investigating the one-step laser lift-off process to facilitate mass production of large area flexible LIBs for self-powered energy sources (Figure S5, Supporting Information) and commercial flexible displays (Figures S5 and S6, Supporting Information).

■ ASSOCIATED CONTENT

📄 Supporting Information

Additional information on the schematics of the fabrication procedures for flexible thin-film LIBs, FEA simulation analysis to evaluate the bending effects of a LIB, film stresses from substrate-delamination and substrate-bending, implementation of an OLED device, fully functional flexible systems, and laser lift-off process for flexible LIBs. Video S1 showing lighting up a commercial blue-LED and voltage retention test of flexible battery. This material is available free of charge via the Internet at <http://pubs.acs.org>.

■ AUTHOR INFORMATION

Corresponding Author

*E-mail: keonlee@kaist.ac.kr. Phone: 82-42-350-3343. Fax: 82-42-350-3310.

Notes

The authors declare no competing financial interest.

■ ACKNOWLEDGMENTS

This research was supported by Basic Science Research Program (CAFDC-2012-0000824, 2012R1A2A1A03010415), World Class University Program (WCU-R32-10051), and Smart IT Convergence System of Global Frontier Project (SIRC-2011-0031848) funded by MEST through the National Research Foundation of Korea (NRF). M.K. thanks Prof. Soo-Il Pyun at KAIST and Dr. Sang-Cheol Nam at GS Nanotech. Co., Ltd. for valuable information related to battery electrochemistry.

■ REFERENCES

- (1) Nishide, H.; Oyaizu, K. *Science* **2008**, *319*, 737–738.
- (2) Jeong, G.; Kim, Y. U.; Kim, H.; Kim, Y. J.; Sohn, H. J. *Energy Environ. Sci.* **2011**, *4*, 1986–2002.
- (3) Lee, S. Y.; Park, K.-I.; Huh, C.; Koo, M.; Yoo, H. G.; Kim, S.; Ah, C. S.; Sung, G. Y.; Lee, K. J. *Nano Energy* **2012**, *1*, 145–151.
- (4) Kim, R. H.; Kim, D.-H.; Xiao, J.; Kim, B. H.; Park, S. I.; Panilaitis, B.; Ghaffari, R.; Yao, J.; Li, M.; Liu, Z.; Malyarchuk, V.; Kim, D. G.; Le, A. P.; Nuzzo, R. G.; Kaplan, D. L.; Omenetto, F. G.; Huang, Y.; Kang, Z.; Rogers, J. A. *Nat. Mater.* **2010**, *9*, 929–937.
- (5) Kim, D.-H.; Viventi, J.; Amsden, J. J.; Xiao, J.; Vigeland, L.; Kim, Y.-S.; Blanco, J. A.; Panilaitis, B.; Frechette, E. S.; Contreras, D.; Kaplan, D. L.; Omenetto, F. G.; Huang, Y.; Hwang, K.-C.; Zakin, M. R.; Litt, B.; Rogers, J. A. *Nat. Mater.* **2010**, *9*, 511–517.

- (6) Lacour, S. P.; Benmerah, S.; Tarte, E.; FitzGerald, J.; Serra, J.; McMahon, S.; Fawcett, J.; Graudejus, O.; Yu, Z.; Morrison, B., 3rd. *Med. Biol. Eng. Comput.* **2010**, *48*, 945–954.
- (7) Kim, S.; Jeong, H. Y.; Kim, S. K.; Choi, S. Y.; Lee, K. J. *Nano Lett.* **2011**, *11*, 5438–5442.
- (8) Lee, C. H.; Kim, D. R.; Zheng, X. L. *Nano Lett.* **2011**, *11*, 3435–3439.
- (9) Lee, C. H.; Kim, D. R.; Zheng, X. L. *Proc. Natl. Acad. Sci. U.S.A.* **2010**, *107*, 9950–9955.
- (10) Abad, E.; Zampolli, S.; Marco, S.; Scorzoni, A.; Mazzolai, B.; Juarros, A.; Gomez, D.; Elmi, I.; Cardinali, G. C.; Gomez, J. M.; Palacio, F.; Cicioni, M.; Mondini, A.; Becker, T.; Sayhan, I. *Sens. Actuators, B* **2007**, *127*, 2–7.
- (11) Scrosati, B. *Nature* **1995**, *373*, 557–558.
- (12) Hu, L.; Choi, J. W.; Yang, Y.; Jeong, S.; La Mantia, F.; Cui, L. F.; Cui, Y. *Proc. Natl. Acad. Sci. U.S.A.* **2009**, *106*, 21490–21494.
- (13) Hu, L.; Pasta, M.; Mantia, F. L.; Cui, L.; Jeong, S.; Deshazer, H. D.; Choi, J. W.; Han, S. M.; Cui, Y. *Nano Lett.* **2010**, *10*, 708–714.
- (14) Jabbour, L.; Gerbaldi, C.; Chaussy, D.; Zeno, E.; Bodoardo, S.; Beneventi, D. *J. Mater. Chem.* **2010**, *20*, 7344–7347.
- (15) Pushparaj, V. L.; Shaijumon, M. M.; Kumar, A.; Murugesan, S.; Ci, L.; Vajtai, R.; Linhardt, R. J.; Nalamasu, O.; Ajayan, P. M. *Proc. Natl. Acad. Sci. U.S.A.* **2007**, *104*, 13574–13577.
- (16) Wu, M. S.; Lee, J. T.; Chiang, P. C. J.; Lin, J. C. *J. Mater. Sci.* **2007**, *42*, 259–265.
- (17) Wei, D.; Andrew, P.; Yang, H. F.; Jiang, Y. Y.; Li, F. H.; Shan, C. S.; Ruan, W. D.; Han, D. X.; Niu, L.; Bower, C.; Ryhanen, T.; Rouvala, M.; Amaratunga, G. A. J.; Ivaska, A. J. *J. Mater. Chem.* **2011**, *21*, 9762–9767.
- (18) Gwon, H.; Kim, H. S.; Lee, K. U.; Seo, D. H.; Park, Y. C.; Lee, Y. S.; Ahn, B. T.; Kang, K. *Energy Environ. Sci.* **2011**, *4*, 1277–1283.
- (19) Nam, K. T.; Kim, D. W.; Yoo, P. J.; Chiang, C. Y.; Meethong, N.; Hammond, P. T.; Chiang, Y. M.; Belcher, A. M. *Science* **2006**, *312*, 885–888.
- (20) Hu, L.; Wu, H.; La Mantia, F.; Yang, Y.; Cui, Y. *ACS Nano* **2010**, *4*, 5843–5848.
- (21) Yang, Y.; Jeong, S.; Hu, L.; Wu, H.; Lee, S. W.; Cui, Y. *Proc. Natl. Acad. Sci. U.S.A.* **2011**, *108*, 13013–13018.
- (22) Sides, C. R.; Li, N. C.; Patrissi, C. J.; Scrosati, B.; Martin, C. R. *MRS Bull.* **2002**, *27*, 604–607.
- (23) Arico, A. S.; Bruce, P.; Scrosati, B.; Tarascon, J. M.; Van Schalkwijk, W. *Nat. Mater.* **2005**, *4*, 366–377.
- (24) Arbizzani, C.; Gabrielli, G.; Mastragostino, M. *J. Power Sources* **2011**, *196*, 4801–4805.
- (25) Barker, J.; Pynenburg, R.; Koksang, R.; Saidi, M. Y. *Electrochim. Acta* **1996**, *41*, 2481–2488.
- (26) Aurbach, D.; Markovsky, B.; Rodkin, A.; Levi, E.; Cohen, Y. S.; Kim, H. J.; Schmidt, M. *Electrochim. Acta* **2002**, *47*, 4291–4306.
- (27) Pistoia, G.; Antonini, A.; Rosati, R.; Zane, D. *Electrochim. Acta* **1996**, *41*, 2683–2689.
- (28) Sans, J. A.; Segura, A.; Mollar, M.; Mari, B. *Thin Solid Films* **2004**, *453*, 251–255.
- (29) Rudenko, A. N.; Keil, F. J.; Katsnelson, M. I.; Lichtenstein, A. I. *Phys. Rev. B* **2011**, *83*, 045409.
- (30) Pyun, S.-I.; Shin, H.-C.; Lee, J.-W.; Go, J.-Y. *Electrochemistry of Insertion Materials for Hydrogen and Lithium*; Springer: Berlin, 2012; ISBN 978-3-642-29463-1.
- (31) Kim, D.-H.; Ahn, J. H.; Choi, W. M.; Kim, H. S.; Kim, T. H.; Song, J. Z.; Huang, Y. G. Y.; Liu, Z. J.; Lu, C.; Rogers, J. A. *Science* **2008**, *320*, 507–511.
- (32) Park, S. I.; Le, A. P.; Wu, J. A.; Huang, Y. G.; Li, X. L.; Rogers, J. A. *Adv. Mater.* **2010**, *22*, 3062–3066.
- (33) Park, M. S.; Hyun, S. H.; Nam, S. C. *J. Power Sources* **2006**, *159*, 1416–1421.
- (34) Hayashi, M.; Takahashi, M.; Sakurai, Y. *J. Power Sources* **2007**, *174*, 990–995.
- (35) Pan, H. J.; Yang, Y. *J. Power Sources* **2009**, *189*, 633–637.
- (36) Yoon, Y. S.; Lee, S. H.; Cho, S. B.; Nam, S. C. *J. Electrochem. Soc.* **2011**, *158*, A1313–A1319.
- (37) Takehara, Z. *J. Power Sources* **1997**, *68*, 82–86.
- (38) Pereira, T.; Scaffaro, R.; Guo, Z.; Nieh, S.; Arias, J.; Hahn, H. T. *Adv. Eng. Mater.* **2008**, *10*, 393–399.
- (39) Stoney, G. G. *Proc. R. Soc. London, Ser. A* **1909**, *82*, 172–175.
- (40) Orman, H. J.; Wiseman, P. J. *Acta Crystallogr., Sect. C* **1984**, *40*, 12–14.
- (41) Mendiboure, A.; Delmas, C.; Hagenmuller, P. *Mater. Res. Bull.* **1984**, *19*, 1383–1392.
- (42) Park, K.-I.; Xu, S.; Liu, Y.; Hwang, G. T.; Kang, S. J. L.; Wang, Z. L.; Lee, K. J. *Nano Lett.* **2010**, *10*, 4939–4943.
- (43) Park, K.-I.; Lee, M.; Liu, Y.; Moon, S.; Hwang, G. T.; Zhu, G.; Kim, J. E.; Kim, S. O.; Kim, D. K.; Wang, Z. L.; Lee, K. J. *Adv. Mater.* **2012**, *24*, 2999–3004.